Gas-phase reactions of atomic lanthanide cations with methyl fluoride: periodicities reactivity

Gregory K. Koyanagi, Xiang Zhao, Voislav Blagojevic, Michael J.Y. Jarvis, Diethard K. Bohme*

Department of Chemistry, Centre for Research in Mass Spectrometry and Centre for Research in Earth and Space Science, York University, Toronto, Ont., Canada M3J 1P3

Dedicated to Bill Hase on the occasion of his 60th birthday in celebration and in recognition of his many outstanding contributions to gas-phase ion chemistry.

Abstract

Room temperature reactions of atomic lanthanide cations (excluding Pm^+) with CH_3F have been surveyed systematically in the gas phase using an inductively-coupled plasma/selected-ion flow tube (ICP/SIFT) tandem mass spectrometer to measure rate coefficients and product distributions in He at 0.35 Torr and 295 K. F-atom transfer was the predominant reaction channel and exhibits increasing efficiency with increasing exothermicity. Minor CH_3F addition was observed with the late lanthanide cations that react slowly. The reaction efficiency for F-atom transfer appears to be governed by the energy required to promote an electron to achieve a d^1s^1 excited electronic configuration in which two non-f electrons are available for bonding: it decreases as the promotion energy increases and the periodic trend in reaction efficiency along the lanthanide series matches the periodic trend in the corresponding electron-promotion energy. This behaviour is consistent with a C−F bond insertion mechanism of the type proposed previously for insertion reactions of Ln^+ cations with hydrocarbons. Direct F-atom abstraction by a harpoon-like mechanism was excluded because of an observed non-correlation of reaction efficiency with $IE(Ln^+)$. A remarkable Arrhenius-like correlation is observed for the dependence of reactivity on promotion energy: the early and late lanthanide cations exhibit characteristic temperatures of 18,000 and 4400 K, respectively. A rapid second F-atom transfer occurs with LaF^+, CeF^+, GdF^+, TbF^+ and LuF^+, but there was no evidence for a third fluorine-atom abstraction with any of the LnF_2^+ cations. Both LnF^+ and LnF_2^+ can add methyl fluoride molecules under the experimental operating conditions of the ICP/SIFT tandem mass spectrometer.
© 2004 Elsevier B.V. All rights reserved.

1. Introduction

Chemical bond activation by atomic ions has become a central theme in gas-phase ion chemistry. Investigations into this type of bond activation began in the early 1980s as soon as suitably versatile sources, in particular, laser ablation/ionization sources, became available for atomic transition-metal ions [1–5]. The measurements were quickly extended to lanthanide cations, Ln^+, and early on in 1988, Schilling and Beauchamp proposed that electron promotion

from the $4f^n6s^1$ ground state to the $4f^{n-1}5d^16s^1$ excited state was required for these cations to be effective in C−H and C−C bond activation and insertion [6]. A plethora of investigations into lanthanide ion chemistry followed, in part to further characterize this requirement, but also motivated by general interests in the gas phase and solution chemistry of lanthanides [7]. Reactions of Ln^+ cations now have been investigated systematically with various inorganic and organic molecules, including hydrogen [8], oxygen [9], nitrous oxide [9], alkanes and cycloalkanes [6,10,11], alkenes [6,12,13], alcohols [14–16], benzene and substituted benzenes [17,18], phenol [19], orthoformates [20], ferrocene [17] and Fe pentacarbonyl [21]. Generally, these studies show that the reactivity of Ln^+ varies along the 4f series, both in terms of

* Corresponding author. Tel.: +1 416 7362100x66188;
fax: +1 416 7365936.
E-mail address: dkbohme@yorku.ca (D.K. Bohme).

the ionic products formed and of the reaction efficiencies. In some instances, the observed trends in reactivity appear to be determined by the accessibility, through electron promotion, of excited electronic configurations of the Ln^+ cation with two unpaired non-f electrons. The results with N_2O also have revealed intriguing Arrhenius-like dependencies of the reactivity of the Ln^+ cation on the electron-promotion energy which exhibit characteristic temperatures of 22,000 and 6100 K for the early and late lanthanide cations, respectively [9].

C–F bond activation, has been the focus in a systematic study of the gas-phase reactivity of the fluorinated hydrocarbons CF_4, CHF_3, CH_3F, C_2F_6, 1,1-$C_2H_4F_2$, and C_6F_6 with the lanthanide cations Ce^+, Pr^+, Sm^+, Ho^+, Tm^+, and Yb^+ and the reactivity of C_6H_5F with all the lanthanide cations except Pm^+ by Fourier-transform ion cyclotron resonance mass spectrometry [22]. Empirical correlations with the second ionization energy of Ln were presented in this study that suggest a "harpoon"-like mechanism for the F-atom abstraction process in which an electron is transferred from the lanthanide cation to the fluorinated substrate in the encounter complex to form $Ln^{2+}F^-$ [22,23]. The F-atom abstraction mechanism has also been studied theoretically for the reactions with Ce^+ and Ho^+ [24] and Ce^+, Pr^+ and Yb^+ [25,26]. Although the calculations were somewhat restrictive, they were interpreted to be consistent with the direct harpoon-type fluorine abstraction mechanism suggested on the basis of the observed empirical correlation.

Here, we have expanded the CH_3F reactivity studies to all the lanthanide cations except Pm^+ using an inductively-coupled plasma/selected-ion flow tube (ICP/SIFT) tandem mass spectrometry [9,27,28]. The experimental results that were obtained have allowed a re-examination of the mechanism of F-atom transfer with a particular view to the insertion [6] and the "harpoon"-like [22] mechanisms that have been advanced previously.

2. Experimental

The experiments were performed with the ICP/SIFT tandem mass spectrometer that has been described in detail previously [9,27,28]. The atomic ions were generated within an atmospheric-pressure argon plasma at 5500 K fed with a vaporized solution containing the lanthanide salt. The ions emerging from the ICP were injected through a differentially pumped sampling interface into a quadrupole mass filter and, after mass analysis, introduced through an aspirator-like interface into flowing helium carrier gas at 0.35 Torr and 295 ± 2 K. After experiencing about 10^5 collisions with He atoms, the ions were allowed to react with CH_3F added into the flow tube.

The lanthanide ions emerging from the plasma initially have a Boltzmann internal energy distribution characteristic of the plasma temperature. However, these emerging populations are expected to be down-graded during the approxi-

mately 20 ms duration before entry into the reaction region in the flow tube. Energy degradation can occur by radiative decay as well as by collisions with argon atoms and the 10^5 collisions with He before entry into the reaction region. The extent to which quenching of any electronically excited states of the lanthanide cations that may be formed within the ICP is complete is uncertain and could be inferred only indirectly from the observed decays of primary ion signals. The observed semi-logarithmic decays of the reacting lanthanide cations were invariably linear often over as much as four decades of ion depletion and so were indicative of single-state populations. The many collisions with Ar and He between the source and the reaction region should ensure that the atomic ions reach a translational temperature equal to the tube temperature of 295 ± 2 K prior to entering the reaction region.

Reactant and product ions were sampled at the end of the flow tube with a second quadrupole mass filter and were measured as a function of added reactant. The resulting profiles provide information about reaction rate coefficients and product-ion distributions. Rate coefficients for primary reactions were determined with an uncertainty estimated to be less than $\pm 30\%$ from the semi-logarithmic decay of the reactant ion intensity as a function of added reactant.

Methyl fluoride was introduced into the reaction region of the SIFT as a dilute mixture in helium ($\sim 10\%$). The methyl fluoride was obtained commercially and was of high purity (Matheson Gas Products, >99%). Separate measurements with Ar^+ indicated impurity levels for SiF_4 of <0.5% as revealed by the production of SiF_3^+.

3. Results and discussion

The reactions of 14 lanthanide cations were investigated with CH_3F. Both the primary and higher-order chemistries were monitored. Results obtained for the reactions of La^+, Gd^+, Dy^+ and Lu^+ are shown in Fig. 1. Table 1 summarizes the measured rate coefficients, reaction efficiencies and product distributions. The reaction efficiency is taken to be equal to the ratio k/k_c, where k is the experimentally measured rate coefficient and k_c is the capture or collision rate coefficient. k_c was computed using the algorithm of the modified variational transition-state/classical trajectory theory developed by Su and Chesnavich [29] with $\alpha(CH_3F) = 2.97 \times 10^{-24}$ cm^3 [30] and $\mu_D(CH_3F) = 1.858$ D [31].

Only F-atom transfer, reaction (1a), and adduct formation, reaction (1b), were observed as primary reaction channels.

$$Ln^+ + CH_3F \rightarrow LnF^+ + CH_3 \qquad (1a)$$

$$Ln^+ + CH_3F \rightarrow Ln^+(CH_3F) \qquad (1b)$$
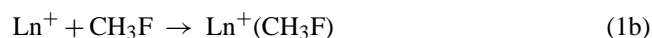
Adduct formation is a minor channel ($\leq 20\%$) and was observed to compete only with the late Ln^+ cations in reactions with low overall reaction efficiencies: those with Dy^+, Ho^+, Er^+, Tm^+, and Yb^+. Reactions with the early lanthanide
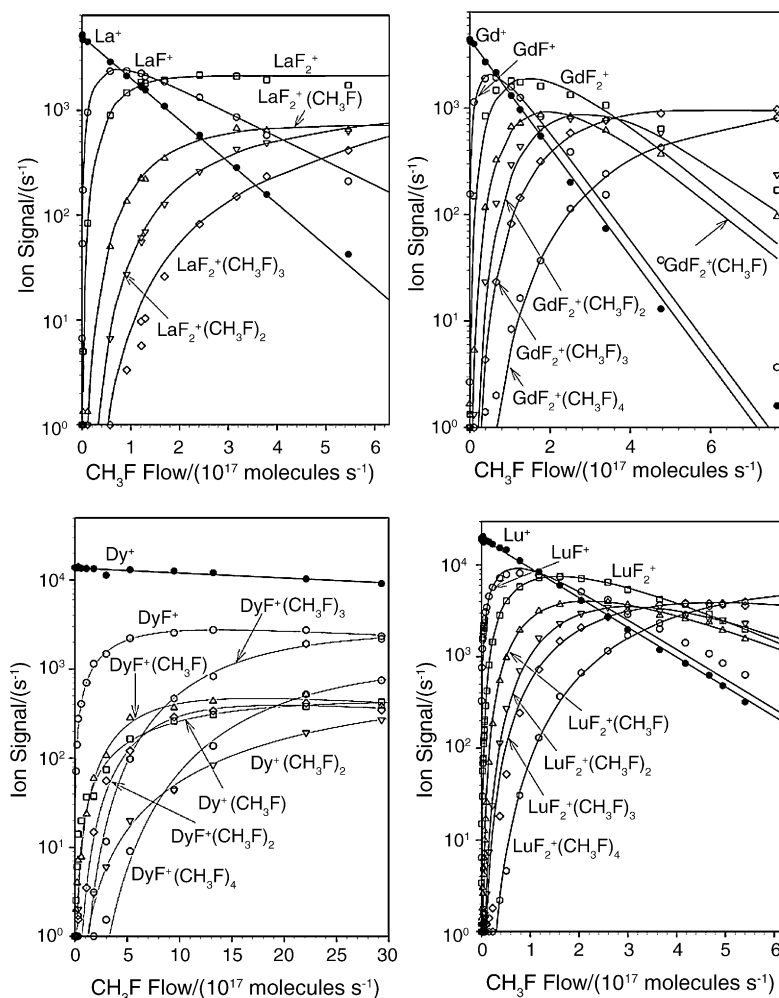
Fig. 1. Composite of ICP/SIFT results for the reactions of the lanthanide metal ions La$^+$, Gd$^+$, Dy$^+$ and Lu$^+$ with CH$_3$F in helium buffer gas at 0.35 ± 0.01 Torr and 295 ± 2 K.

cations exhibited ≤1% adduct formation. As expected from the much lower first ionization energy of the lanthanides, IE(Ln), all <6.3 eV, than that for CH$_3$F (12.47 ± 0.02 eV) [32], electron transfer was not observed with any of the Ln$^+$ cations.

A fast ($k \geq 6 \times 10^{-10}$ cm^3 molecule^{-1} s^{-1}) second fluorine-atom abstraction, reaction (2), was observed with LaF$^+$ (6.3), CeF$^+$ (7.4), GdF$^+$ (11), TbF$^+$ (18) and LuF$^+$ (17).

$$LnF^+ + CH_3F \rightarrow LnF_2^+ + CH_3 \qquad (2)$$
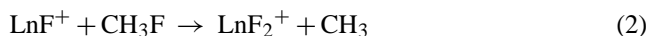
The remaining LnF$^+$ cations react with CH$_3$F with rate coefficients equal to or less than that measured for the first abstraction and with the exception of Ho$^+$ and Er$^+$ (for which LnF$_2^+$ formation was predominant) react primarily (≥90%) by CH$_3$F addition. No third fluorine-atom abstraction was observed with any of the LnF$_2^+$ cations.

CH$_3$F addition according to reaction (3) also was observed for almost all of the lanthanide fluoride cations. These addi-

tion reactions are expected to be termolecular with He buffer-gas atoms acting as the stabilizing third body.

$$LnF_m^+(CH_3F)_n + CH_3F \rightarrow LnF_m^+(CH_3F)_{n+1}$$

$$(m = 0\text{--}2) \qquad (3)$$
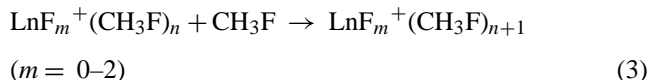
Secondary and higher-order CH$_3$F addition was observed for LnF$^+$ = HoF$^+$ ($m = 1, n = 0$), YbF$^+$ ($m = 1, n = 0$–1), PrF$^+$, NdF$^+$ ($m = 1, n = 0$–2), SmF$^+$, EuF$^+$, DyF$^+$, HoF$^+$, ErF$^+$, TmF$^+$ ($m = 1, n = 0$–3), and LnF$_2^+$ = LaF$_2^+$, CeF$_2^+$ ($m = 2$, $n = 0$–2), GdF$_2^+$, TbF$_2^+$, HoF$_2^+$, ErF$_2^+$, TmF$_2^+$, LuF$_2^+$ ($m = 2, n = 0$–3). Table 1 includes a listing of all the higher-order product ions that were observed. The higher-order chemistry initiated by La$^+$, Gd$^+$, Dy$^+$ and Lu$^+$ can be tracked in Fig. 1.

The possible role of impurity SiF$_4$ (determined to be <0.5% from our chemical ionization measurement with Ar$^+$) as a source of F in a possible F-atom transfer reaction with SiF$_4$ can be excluded on the basis of the very strong

Table 1
Primary reaction rate coefficients (in 10^{-10} cm^3 molecule^{-1} s^{-1}), reaction efficiencies (k/k_c), primary product distributions and higher-order product ions measured for reactions of atomic cations Ln$^+$ with CH$_3$F in helium at 0.35 ± 0.01 Torr and 295 ± 2 K

M$^+$	k[a]	k_c[b]	k/k_c	Primary products	PD[c]	Higher-order product ions
La$^+$	4.5	18.6	0.24	LaF$^+$	100	LaF$_2^+$, LaF$_2^+$(CH$_3$F)$_{1-3}$
Ce$^+$	3.8	18.6	0.20	CeF$^+$	100	CeF$_2^+$, CeF$^+$(CH$_3$F), CeF$_2^+$(CH$_3$F)$_{1-3}$
Pr$^+$	1.4	18.6	0.075	PrF$^+$	100	PrF$_2^+$, PrF$^+$(CH$_3$F)$_{1-3}$
Nd$^+$	1.4	18.6	0.073	NdF$^+$	100	NdF$^+$(CH$_3$F)$_{1-3}$
Sm$^+$	0.56	18.5	0.030	SmF$^+$	100	SmF$^+$(CH$_3$F)$_{1-4}$
Eu$^+$	0.35	18.4	0.019	EuF$^+$	100	EuF$^+$(CH$_3$F)$_{1-4}$
Gd$^+$	6.9	18.4	0.37	GdF$^+$	100	GdF$_2^+$, GdF$_2^+$(CH$_3$F)$_{1-4}$
Tb$^+$	1.9	18.4	0.10	TbF$^+$	100	TbF$_2^+$, TbF$_2^+$(CH$_3$F)$_{1-4}$
Dy$^+$	0.070	18.3	3.8×10^{-3}	DyF$^+$	~95	DyF(CH$_3$F)$_{1-4}$
				Dy$^+$CH$_3$F	~5	Dy$^+$(CH$_3$F)$_2$
Ho$^+$	0.075	18.3	4.1×10^{-3}	HoF$^+$	~95	HoF$_2^+$, HoF$^+$(CH$_3$F), HoF$_2^+$(CH$_3$F)$_{1-4}$
				Ho$^+$CH$_3$F	~5	Ho$^+$(CH$_3$F)$_2$
Er$^+$	0.094	18.3	5.1×10^{-3}	ErF$^+$	~90	ErF$_2^+$, ErF$_2^+$(CH$_3$F)$_{1-4}$
				Er$^+$CH$_3$F	~10	Er$^+$(CH$_3$F)$_2$
Tm$^+$	≤0.01	18.3	$\leq 5.0 \times 10^{-4}$	TmF$^+$	~80	TmF$_2^+$, TmF$_{1,2}^+$(CH$_3$F)$_{1-4}$
				Tm$^+$CH$_3$F	~20	Tm$^+$(CH$_3$F)$_2$
Yb$^+$	≤0.01	18.2	$\leq 5.0 \times 10^{-4}$	YbF$^+$	~90	YbF$^+$(CH$_3$F)$_{1-2}$
				Yb$^+$CH$_3$F	~10	
Lu$^+$	6.7	18.2	0.37	LuF$^+$	100	LuF$_2^+$, LuF$_2^+$(CH$_3$F)$_{1-4}$

Also included are calculated collision rate coefficients, k_c (in 10^{-10} cm^3 molecule^{-1} s^{-1}) and reaction efficiencies, k/k_c (see text).

  [a] Measured reaction rate coefficient with an estimated accuracy of ±30%.
  [b] Calculated capture rate coefficient (see text).
  [c] PD = product distribution expressed as a percentage.

F–SiF$_3$ bond, FA(SiF$_3$) = 166 ± 5 kcal mol^{-1} [32]. Table 2 shows that the F-atom affinities of the Ln$^+$ cations (Dy$^+$, Ho$^+$, Er$^+$) that react by F-atom abstraction with efficiencies of ca. 0.5% are all at least 23 kcal mol^{-1} lower (tak-

ing into account uncertainties) than FA(SiF$_3$) but higher than FA(CH$_3$) = 113 kcal mol^{-1} [32].

3.1. Periodicities in reaction efficiencies

The primary reaction efficiencies of the 14 Ln$^+$ cations with CH$_3$F change dramatically along the 4f row. The efficiencies of the reactions of La$^+$ (0.24), Ce$^+$ (0.20), Gd$^+$ (0.37), Tb$^+$ (0.10) and Lu$^+$ (0.37) are all higher than 0.10 and it is interesting to note that these cations (except Tb$^+$) have two non-f electrons in their electronic ground state. In contrast, the efficiencies of the reactions of the early lanthanide cations Pr$^+$ (0.075), Nd$^+$ (0.073), Sm$^+$ (0.030), and Eu$^+$ (0.019) are all ≤0.075 and those of the late lanthanide cations Dy$^+$ (0.0038), Ho$^+$ (0.0041), Er$^+$ (0.0051), Tm$^+$ (0.0007), and Yb$^+$ (0.0054) are all ≤0.005, near the detection limit. An overview of the variation in reaction efficiency across the lanthanide series is included in Fig. 2.

3.2. Thermodynamics of F-atom abstraction

F-atom abstraction was observed with all the lanthanide cations. Rate coefficients measured for F-atom abstraction are in the range ≤1.0×10^{-12} cm^3 molecule^{-1} s^{-1} (for Tm$^+$ and Yb$^+$) to 6.9×10^{-10} cm^3 molecule^{-1} s^{-1} (for Gd$^+$). Assuming that only exothermic or thermoneutral reaction can be observed under our experimental operating conditions, we estimate that the fluorine-atom affinity, FA(Ln$^+$), is higher than FA(CH$_3$) = 113 kcal mol^{-1} [32] for all the lanthanide

Table 2
Fluorine atom affinities, FA (in kcal mol^{-1}), and selected electronic properties (in kcal mol^{-1}) for lanthanide cations

Ln$^+$ species	FA(Ln$^+$)	Ln$^+$ ground state valence configuration	Ln$^+$ term symbol[a]	Promotion energy to first 5d^{1}6s^1 configuration[a]
La$^+$	174.9[b]	5d^2	$^3F_2$	4.5 ± 3.0
Ce$^+$	151.2[c]	4f^{1}5d^2	$^4H_{7/2}^0$	4.6 ± 5.7
Pr$^+$	138.3[c]	4f^{3}6s^1	(9/2, 1/2)$_4^0$	22.3 ± 0.8
Nd$^+$	143 ± 7[d]	4f^{4}6s^1	$^6I_{7/2}$	34.8 ± 8.3
Pm$^+$		4f^{5}6s^1	$^7H_2^0$	46.4 ± 7.2
Sm$^+$	130 ± 7[d]	4f^{6}6s^1	$^8F_{1/2}$	62.1 ± 5.8
Eu$^+$		4f^{7}6s^1	$^9S_4^0$	92.8 ± 5.0
Gd$^+$		4f^{7}5d^{1}6s^1	$^{10}D_{5/2}^0$	0.0
Tb$^+$		4f^{9}6s^1	(15/2, 1/2)$_8^0$	9.3 ± 8.1
Dy$^+$	125 ± 7[d]	4f^{10}6s^1	(8, 1/2)$_{17/2}$	36.0 ± 6.1
Ho$^+$	129.8[e] 127 ± 7[d]	4f^{11}6s^1	(15/2, 1/2)$_8^0$	37.8 ± 5.4
Er$^+$	131 ± 7[d]	4f^{12}6s^1	(6, 1/2)$_{13/2}$	34.5 ± 3.1
Tm$^+$		4f^{13}6s^1	(7/2, 1/2)$_4^0$	55.5 ± 7.4
Yb$^+$	123.6[c]	4f^{14}6s^1	$^2S_{1/2}$	79.4 ± 4.0
Lu$^+$		4f^{14}6s^2	$^1S_0$	36.6 ± 3.6

  [a] See [9].
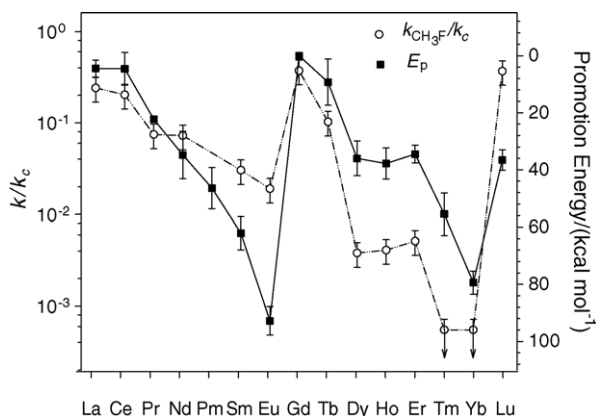 [b] See [25].
  [c] See [26].
  [d] See [22].
  [e] See [33].

Fig. 2. Reaction efficiency (open circles and left ordinate axis) and the energy required to promote an electron and leave the Ln^+ cation in a d^1s^1 configuration (solid squares and right ordinate axis) plotted along the lanthanide row of elements. There is an apparent correlation between reaction efficiency and electron-promotion energy.

cations investigated. The nine F-atom affinities available either from theory or from experiment are included in Table 2. All of these values are $>113\,kcal\,mol^{-1}$ and so the F-atom abstraction reactions with all of these lanthanide cations are exothermic (by $>10\,kcal\,mol^{-1}$). Fig. 3 shows how the reaction efficiency for F-atom transfer varies with the F-atom affinity for the nine lanthanide cations with known values of $FA(Ln^+)$. There appears to be a shift of ca. $10\,kcal\,mol^{-1}$ in the onset of exothermic F-atom transfer which exhibits increasing efficiency with increasing exothermicity.

3.3. Mechanism for F-atom abstraction by Ln^+

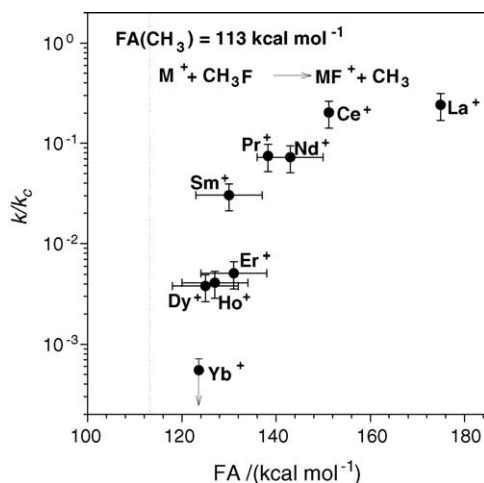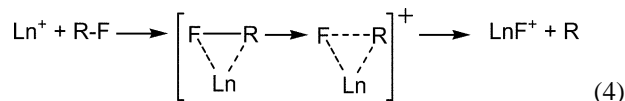Two possible mechanisms have been advanced for F-atom abstraction reactions of Ln^+ cations with fluorinated hydrocarbons [22]:

Fig. 3. Dependence of the reaction efficiency for F-atom transfer, k/k_c, on the F-atom affinity, FA, of the lanthanide cation, $FA(Ln^+)$. k represents the measured reaction rate coefficient and k_c is the calculated collision rate coefficient (see Table 1). All reactions (on the right of the dashed line) are exothermic for F-atom abstraction.

- Mechanism I: insertion-elimination, Eq. (4).
  In this mechanism, a three-membered cyclic ion complex is initially formed and then transformed through a three-centre transition state into a complex in which Ln^+ is inserted into the R–F bond. The inserted complex can then eliminate the LnF^+ and R species. R–F bond insertion in the reaction with Pr^+ has been viewed to occur via an "avoided crossing" of two hypersurfaces corresponding to the Pr^+ ground state and an excited state of a valence configuration with two non-f electrons to yield F–Pr^+–R which eliminates an R radical [34]. It has been shown previously that this mechanism applies to hydrocarbon activation by Ln^+ [10].

$$Ln^+ + R\text{-}F \longrightarrow \left[\begin{array}{c} F\text{---}R \\ \diagdown\ \diagup \\ Ln \end{array} \longrightarrow \begin{array}{c} F\text{----}R \\ \diagdown \\ Ln \end{array} \right]^+ \longrightarrow LnF^+ + R \tag{4}$$

- Mechanism II: a "harpoon"-like mechanism, Eq. (5).
  This mechanism involves the transfer of an electron within the encounter complex $LnFR^+$, perhaps at long range, from the lanthanide cation to the fluorinated substrate. This favours the homolytic cleavage of the C–F bond to form LnF^+.

$$Ln^+ + R\text{–}F \rightarrow [Ln^+ \cdots F\text{–}R$$
$$\rightarrow Ln^{2+}\text{–}F^- \cdots R] \rightarrow LnF^+ + R \tag{5}$$
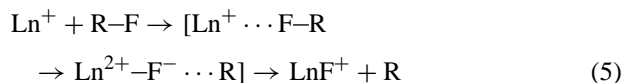
While the two mechanisms are unlikely to be distinguishable on the basis of rate measurements alone, they do differ in the expected correlations of reaction efficiencies with specific physical properties of the Ln^+ cations. Thus, mechanism II might exhibit a correlation of reaction efficiency with the second ionization energy of Ln, $IE(Ln^+)$, as has been proposed by Cornehl et al. [22] in their attempt to account for their measured reaction rates with fluoromethane, 1,1-difluoroethane, fluorobenzene, and hexafluorobenzene. Their measurements with CH_3F showed this expected correlation but were restricted to a set of only six lanthanide cations: Ce^+, Pr^+, Sm^+, Ho^+, Tm^+, and Yb^+.

However, our experimental results show that the ability of Ln^+ to abstract a fluorine atom from methyl fluoride does not correlate well with the second IE of the lanthanide (see Fig. 4); $IE(Ln^+)$ (eV) = La^+ (11.06), Ce^+ (10.85), Pr^+ (10.55), Nd^+ (10.72), Sm^+ (11.07), Eu^+ (11.25), Gd^+ (12.10) Tb^+ (11.52), Dy^+ (11.67), Ho^+ (11.80), Er^+ (11.93), Tm^+ (12.05), Yb^+ (12.17), and Lu^+ (13.9) [35]. So we cannot assign mechanism II to these reactions with CH_3F on the basis of such a correlation. The assertion by Cornehl et al. [22] that this mechanism applies is based on too limited a database (their data points are included in Fig. 4). Of course, this does not imply that the harpoon mechanism might not apply to the other F-atom abstraction reactions reported by these authors, especially with fluorobenzene for which a strong correlation with $IE(Ln^+)$ was found over *all* the lanthanide cations (except Pm^+) [22]. We propose here that the mechanism for F-atom
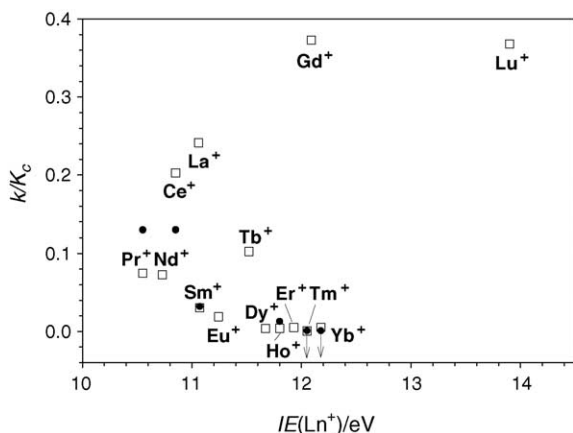
Fig. 4. The dependence of the efficiencies for F-atom abstraction in reactions of Ln^+ with CH_3F on the second ionization energy of Ln, $IE(Ln^+)$. The open squares refer to this work and the solid circles are the results reported by Cornehl et al. [10] adjusted to the same collision rate coefficient (k_c rather than k_{ADO}).
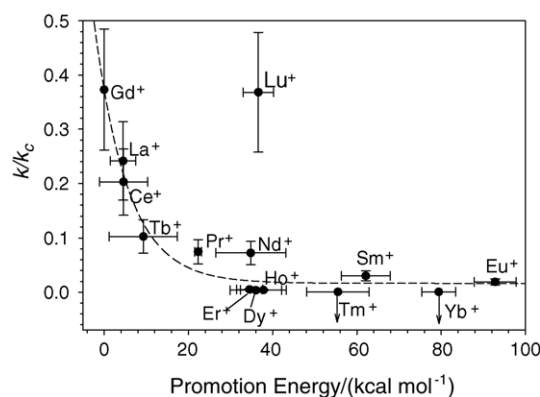

Fig. 5. Correlation of reaction efficiency for F-atom abstraction from CH_3F with the energy E_p required to promote an electron and leave the Ln^+ cation in a d^1s^1 configuration. The dashed curve represents a fit with $k/k_c = 0.016 + 0.36 \exp(-0.13E_p)$.

transfer actually depends on the nature of the fluorocarbon and that the harpoon mechanism is more favourable with fluorobenzene because of the possibility of charge transfer from the π system of the phenyl ring to the incoming Ln^+ cation. Such a transfer of charge will partially neutralize the Ln^+ and so reduce the energy required to release the electron harpoon from Ln^+ to the F atom to a value closer to the first ionization energy of Ln, $IE(Ln)$, which is significantly smaller than $IE(Ln^+)$. This reduces the energy change associated with the electron transfer from the lanthanide cation to the fluorinated substrate and so enhances the probability of electron harpooning. Charge transfer from the methyl substituent to the incoming Ln^+ cation, and therefore the harpoon mechanism, is expected to be much less favourable with methyl fluoride.

Our experimental results suggest that Gd^+ ($4f^75d^16s^1$) with two non-f valence electrons exhibits the highest efficiency for F-atom abstraction followed closely by La^+ ($5d^2$), Ce^+ ($4f^15d^2$) and Lu^+ ($4f^{14}6s^2$) all of which also have two non-f valence electrons. The reactivities of the remaining Ln^+ cations, all of which have available only one non-f electron (s^1), are all less and decrease along the early and late lanthanide series. So apparently the s electron at most plays a small role in determining these reactivities. Indeed, as shown in Figs. 2 and 5, these decreasing reactivities correlate well with the variation in the electron-promotion energy of Ln^+ required to achieve a $4f^{n-1}5d^16s^1$ configuration. Thus, f to d electron promotion appears crucial for the efficient occurrence of F-atom transfer. Also, the relatively high efficiencies of the reactions with La^+ ($5d^2$) and Ce^+ ($4f^15d^2$) are *lower* than that of the reaction with Gd^+ ($4f^75d^16s^1$) and this suggests a further correlation with the d to s promotion energy for these two lanthanide cations. Taken together, these correlations indicate that two non-f electrons in a d^1s^1 configuration are required for F-atom abstraction from CH_3F, the reaction occurs via mechanism I. We note that the trend exhibited in Fig. 5 is remarkably similar to that presented by

Cornehl et al. [10], Fig. 3 for reactions of Ln^+ cations with saturated and unsaturated hydrocarbons for which mechanism I also has been advanced. The small amounts of $Ln^+(CH_3F)$ adduct ions observed with the late lanthanide cations may be collisionally-stabilized remnants of the inserted reaction intermediate.

Lu^+ is an exception since it has a $4f^{14}6s^2$ configuration and a high s to d promotion energy ($36.6 \, kcal \, mol^{-1}$) but nevertheless is quite reactive ($k/k_c = 0.37$). We suggest that this apparent anomaly may be explained by the overlap of the $6s^2$ orbital with the antibonding orbital of methyl fluoride. This will weaken the $F–CH_3$ bond sufficiently to enable F-atom transfer without the need for s to d promotion

Fig. 6 demonstrates, in an Arrhenius-like plot, that the reaction efficiency of the Ln^+ reactions with CH_3F, here measured at constant temperature (295 K), exhibits an ex-
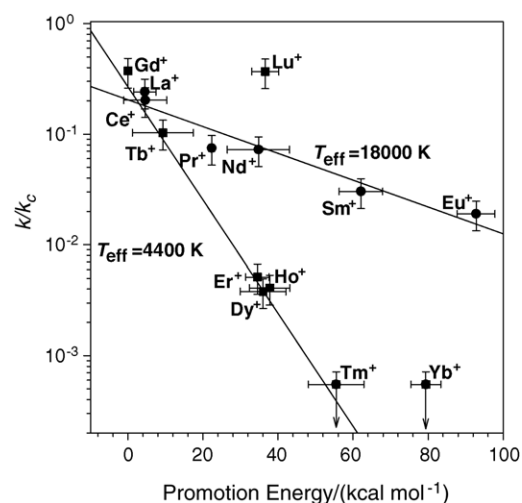

Fig. 6. Arrhenius-like correlation of reaction efficiency for F-atom abstraction from CH_3F with the energy required to promote an electron and leave the Ln^+ cation in a d^1s^1 configuration in the reactions of early and late Ln^+ ions with CH_3F. Lu^+ clearly is an exception to the trend observed for the late Ln^+ ions.

ponential dependence on the promotion energy according to Eq. (6).

$$\frac{k}{k_c} = \exp(-XE_p) \qquad (6)$$

A remarkable aspect of these results is the distinct difference in this dependence between the early and late lanthanide ions. It is interpreted as $1/RT_{eff}$, the slopes of the semi-logarithmic plots in Fig. 6 indicate characteristic temperatures of $18,000 \pm 2400$ and 4400 ± 200 K for F-atom abstraction with the early and late lanthanide cations, respectively. Lu^+ again appears anomalous in that its reactivity is abnormally high. We postulate, as we have done before for reactions of Ln^+ with N_2O [9], that the difference in characteristic temperature possibly can be attributed to the energy associated with the electron promotion. Electron promotion in the early lanthanide ions involves an unpaired f electron while that in the late lanthanide ions involves a paired f electron. Thus, electron promotion in the late lanthanide ions involves electron–electron repulsion and so can be expected to be more effective and exhibit a lower characteristic temperature. It is noteworthy that the characteristic temperatures obtained for the F-atom abstraction from CH_3F with the early and late lanthanide cations are similar to those, 22,000 and 6100 K, respectively, that we have previously obtained for O-atom abstraction from N_2O [9]. This would be expected as we have postulated that both processes require the electronic excitation of Ln^+.

Inspection of our results for the addition of another F atom to LnF^+ in a second reaction with CH_3F indicates that the second F-atom transfers are fast ($k > 6 \times 10^{-10}$ cm^3 molecule^{-1} s^{-1}) with those Ln^+ cations with low promotion energies ($E_p < 9.3$ kcal mol^{-1}) and slow ($k < 2 \times 10^{-11}$ cm^3 molecule^{-1} s^{-1}) with those Ln^+ cations with high promotion energies ($E_p > 22.3$ kcal mol^{-1}) with Lu^+ ($k = 1.7 \times 10^{-9}$ cm^3 molecule^{-1} s^{-1}, $E_p = 36.6$ kcal mol^{-1}) again being the exception. Such a reactivity pattern again is not inconsistent with an insertion mechanism that requires two unpaired valence electrons.

4. Conclusions

Lanthanide cations have been observed to react with methyl fluoride at room temperature predominantly by F-atom transfer. The efficiency of this transfer correlates with the energy required to promote an electron to achieve a d^1s^1 excited electronic configuration in which two non-f electrons are available for bonding. The efficiency decreases as the promotion energy increases and the periodic trend in reaction efficiency along the lanthanide series matches the periodic trend in the corresponding electron-promotion energy. This behaviour is consistent with a C−F bond insertion mechanism of the type proposed previously for C−H and C−C bond activation reactions of Ln^+ cations with alkanes and alkenes [10]. Direct F-atom abstraction by a harpoon-like mechanism can

be excluded on the basis of an observed non-correlation of reaction efficiency with IE(Ln^+). A remarkable Arrhenius-like correlation is observed for the dependence of reactivity on promotion energy: the early and late lanthanide cations exhibit characteristic temperatures of 18,000 K and 4400 K, respectively. A rapid second F-atom transfer occurs with LaF^+, CeF^+, GdF^+, TbF^+ and LuF^+ but there was no evidence for a third fluorine-atom abstraction with any of the LnF_2^+ cations. Both LnF^+ and LnF_2^+ can add methyl fluoride molecules under the experimental operating conditions of the ICP/SIFT tandem mass spectrometer.

References

[1] P.B. Armentrout, Annu. Rev. Phys. Chem. 41 (1990) 313.
[2] M. Simões, J.L. Beauchamp, Chem. Rev. 90 (1990) 629.
[3] K. Eller, H. Schwarz, Chem. Rev. 91 (1991) 1121.
[4] J.C. Weisshaar, Acc. Chem. Res. 26 (1993) 213.
[5] B.S. Freiser, Acc. Chem. Res. 27 (1994) 353.
[6] J.B. Schilling, J.L. Beauchamp, J. Am. Chem. Soc. 110 (1988) 15.
[7] D.K. Bohme, Gas-phase reactivity of lanthanide cations, in: M.L. Gross, R. Caprioli (Eds.), Encyclopedia of Mass Spectrometry, vol. 4, Elsevier, New York, 2004, pp. 638–648.
[8] J.L. Elking, L.S. Sunderlin, P.B. Armentrout, J. Phys. Chem. 93 (1989) 3151.
[9] G.K. Koyanagi, D.K. Bohme, J. Phys. Chem. A 105 (2001) 8964.
[10] H.H. Cornehl, C. Heinemann, D. Schroder, H. Schwarz, Organometallics 14 (1995) 992.
[11] L.S. Sunderlin, P.B. Armentrout, J. Am. Chem. Soc. 111 (1989) 3845.
[12] Y. Huang, M.B. Wise, D.B. Jacobson, B.S. Freiser, Organometallics 6 (1987) 346.
[13] J.K. Gibson, J. Phys. Chem. 100 (1996) 15688.
[14] M. Azzaro, S. Breton, M. Decouzon, S. Geribaldi, Int. J. Mass Spectrom. Ion Processes 128 (1993) 1.
[15] S. Geribaldi, S. Breton, M. Decouzon, M. Azzaro, J. Am. Soc. Mass Spectrom. 7 (1996) 1151.
[16] J.M. Carretas, J. Marcalo, A. Pires de Matos, Int. J. Mass Spectrom. 234 (2004) 51.
[17] J.K. Gibson, R.G. Haire, Radiochim. Acta 89 (2001) 709.
[18] W.W. Yin, A.G. Marshall, J. Marcalo, A.N. Pires de Matos, J. Am. Chem. Soc. 116 (1994) 8666.
[19] J.M. Carretas, A.P. de Matos, J. Marcalo, M. Pissavini, M. Decouzon, S. Geribaldi, J. Am. Soc. Mass Spectrom. 9 (1998) 1035.
[20] N. Marchande, S. Breton, S. Geribaldi, J.M. Carretas, A.P. de Matos, J. Marcalo, Int. J. Mass Spectrom. 195–196 (2000) 139.
[21] M. da Conceicao Vieira, J. Marcalo, A. Pires de Matos, J. Organomet. Chem. 632 (2001) 126.

[22] H.H. Cornehl, G. Hornung, H. Schwarz, J. Am. Chem. Soc. 118 (1996) 9960.

[23] U. Mazurek, H. Schwarz, Chem. Comm. (2003) 1321.

[24] R.H. Hertwig, W. Koch, Chem. Eur. J. 5 (1999) 312.

[25] D. Zhang, C. Zhang, C. Liu, J. Organomet. Chem. 640 (2001) 121.

[26] D. Zhang, C. Liu, S. Bi, J. Phys. Chem. A 106 (2002) 4153.

[27] G.K. Koyanagi, V.V. Lavrov, V. Baranov, D. Bandura, S. Tanner, J.W. McLaren, D.K. Bohme, Int. J. Mass Spectrom. 194 (2000) L1.

[28] G.K. Koyanagi, V. Baranov, S. Tanner, D.K. Bohme, Anal. At. Spectrom. 15 (2000) 1207.

[29] T. Su, W.J. Chesnavich, J. Chem. Phys. 76 (1982) 5183.

[30] H. Sutter, R.H. Cole, J. Chem. Phys. 52 (1970) 132.

[31] D.R. Lide, CRC Handbook of Chemistry and Physics, 80th ed., CRC Press, 2001.

[32] S.G. Lias, J.E. Bartness, J.F. Liebman, J.L. Holmes, R.D. Levin, W.G. Mallard, J. Phys. Chem. Ref. Data 17 (Suppl. 1) (1988).

[33] J.K. Gibson, J. Fluorine Chem. 78 (1996) 65.

[34] C. Heinemann, N. Goldgerg, I. Tornieporth-Oetting, T.M. Klapötke, H. Schwarz, Angew. Chem. Int. Ed. Engl. 34 (1995) 213.

[35] C.E. Moore, Natl. Stand. Ref. Data Ser., Natl. Bur. Stand. 34 (1970).